

# Advanced Visual Inspection Technology with 2-Dimensional Motion Images for Film-shaped Products

Sumitomo Chemical Co., Ltd.  
Industrial Technology & Research Laboratory  
Osamu HIROSE  
Maya OZAKI

This paper presents an advanced technology for visual inspection of film products. Usually, a line sensor is used to inspect defects in web-shape products such as long films. However, one-dimensional image data captured via line sensors always includes restrictive optical information about defects. Therefore, inspection performance is limited. With the advantage of using area sensors, two-dimensional images containing more optical information can be obtained. The authors have established a novel imaging procedure which is based on two-dimensional motion images. The experimental results show that the new image processing framework enhances the appearance of defects. The authors also achieved an in-line web inspection system for film manufacturing lines.

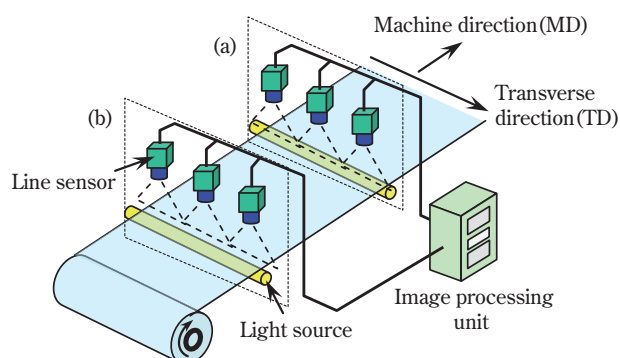
This paper is translated from R&D Report, "SUMITOMO KAGAKU", vol. 2013.

## Introduction

This paper presents a novel visual inspection technology based on two-dimensional motion images. A web inspection system, which has improved functions and inspection performance, has been developed by using two-dimensional motion images obtained by multiple area sensors<sup>1)</sup>.

Usually, line sensors<sup>1)</sup> are adopted to inspect defects in web-shape products such as long films. An image that covers the entire area of the product is acquired by scanning a one-dimensional visual field on the product. Defects such as scratches and foreign matter are extracted from this image. **Fig. 1** shows a typical configuration for the web inspection system. In most cases, by conveying the product below the view of fixed line sensors, the entire area of the product can be inspected. There are various web-shape products, for instance resin film, paper, glass and steel plates, that are capable of being inspected by this method. For simplicity, "film", which denotes one kind of possible web-shape product, is used in the remainder of this paper.

Inspection methods with multiple line sensors have a technical problem in terms of their functions, with which not all kinds of defects with different characteristics can be detected. The main reason is the field of view of the line sensor must be fixed on one dimension-



**Fig. 1** Traditional web inspection system  
Camera group (a) and (b) indicate bright-field mode and dark-field mode respectively.

al region. Since the imaging region is fixed, the optical conditions must also be fixed. Moreover, various types of defects occurring on the actual film products require different optical conditions (for example, with transmitted light or reflected light, bright field imaging or dark field imaging, etc.) to be detected separately. Yet, of all of the optical conditions, merely one specific condition could be selected at any one moment. Therefore, the obtained images contain limited information about some kinds of defects.

In addition, traditional inspection with line sensors has another problem from a practical standpoint. It

requires advanced web handling<sup>3)</sup> techniques to keep inspection performance. High-precision alignment among cameras, the film and the light source is needed to obtain images suitable for defect detection. For example, to inspect optical films assembled into IT devices, positioning accuracy of less than 10 micrometers is generally required. Cameras and light sources are fixed easily with accuracy. However, large-scale web handling equipment and highly skilled techniques for operating them are necessary to convey films with good precision.

These problems with the conventional method mentioned above could be resolved via web inspection techniques by using two-dimensional motion images.

In this research, the authors have proposed a novel image processing algorithm called “line composition and integration (LCI)” which successfully extracted defect information from two-dimensional image sequences, and demonstrated its effectiveness<sup>4)</sup> through experimental results. LCI is a procedure that is able to process various optical conditions, such as from bright fields to dark fields, all at once.

Furthermore, a real-time two-dimensional image processing system was also developed. It is difficult to accomplish real-time processing on the software system, since two-dimensional images contain much more informative data than images captured by line sensors (in this paper, “real-time” means that the image processing time is short enough to keep up with the actual manufacturing speed). For this reason, the authors adopted an image capture board embedded with an FPGA (a type of rewritable large-scale integrated circuit) and installed LCI procedures in the FPGA. As a result, real-time image processing was eventually achieved.

In this paper, the problems with the conventional method are discussed and the merits of using area sensors for solving these problems are introduced. Following that, experimental results are shown. Then, we discuss the computer graphics generation of defect images by light ray trace simulation. Finally an in-line web inspection system is described.

## Problems of Conventional Method

### 1. Typical framework of the web inspection system and its overview

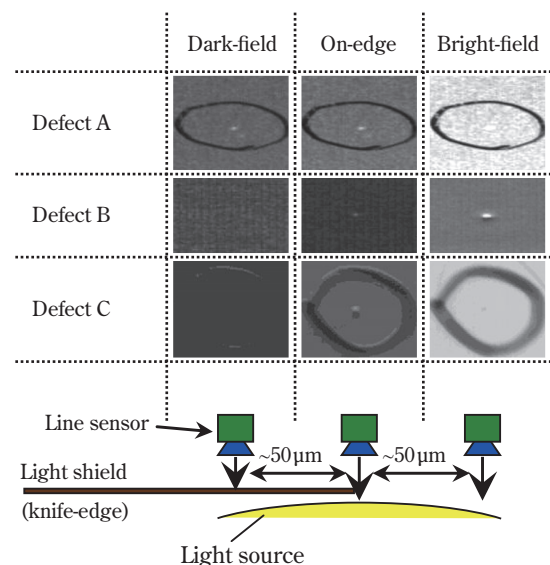
A typical framework of a web inspection system with line sensors was shown in Fig. 1 in the previous chap-

ter. Line sensors are set up to cover the whole width of film. The direction of the imaging region is in the transverse direction (TD) to film conveying. Long film products are transported at almost constant speed in its longitudinal direction (machine direction; MD). The line sensors carry out imaging of the same straight line continuously and repeatedly, so that the film can be imaged over the whole area and inspected while being conveyed. The TD resolution is calculated from the ratio of the field of view divided by the number of pixels involving each camera. Additionally, the MD resolution is determined by the ratio of the conveying speed divided by the scanning rate (number of images made per unit time). The TD and MD resolution are usually adjusted to the same value.

### 2. Technical problems with observation system

The inspection technology based on line sensors has a problem that various types of defects with different properties cannot be imaged by a single observation system. The main reason is that the imaging region of line sensors is fixed at one dimension, so the optical conditions during imaging must also be fixed to one parameter.

On the other hand, the optical conditions suitable for detection differ for each type of defect arising in films. Fig. 2, for example, shows a comparison of defect images captured under different optical conditions by using a transmission light source involving several typical defects. The light source and cameras are set up to



**Fig. 2** Various observation methods for different types of defects

face each other, and a light shield plate that has a linear shaped knife edge is arranged to cover half of the light source area. Three types of optical conditions such as dark field, on-edge and bright field are illustrated in the figure. The dark field means an imaging method in which observations are not made directly from light from the light source; on-edge is a method in which each line sensor is aligned with its imaging region located just on a knife edge, and bright field is a method in which light from the light source is received directly. Among these, defect A is erased by the surrounding light under bright field conditions, but in the dark field or on-edge images, it is clearly imaged. In contrast, defect B can only be observed in the bright field. In addition, with defect C, it is difficult to view the defect in both bright field and dark field, and the defect can only be confirmed in the on-edge image.

When you use line sensors, you need to select one of these optical arrangements and fix the line sensors and light source. Or, multiple inspection systems are needed to cover different types of defects. Fig. 1, described above, is an example of an inspection system consisting of bright field and dark field units set up in two series.

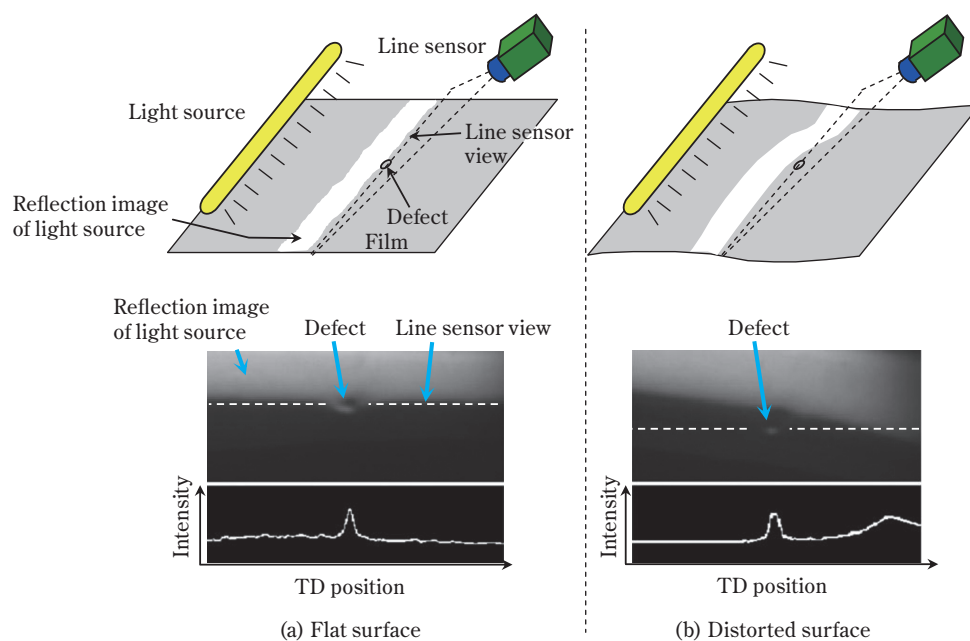
### 3. Precision requirement for web handling technology

Inspection with line sensors has a practical disadvantage in that high precision web handling techniques are

required to maintain inspection performance. The differences in the camera positions among these observation methods, described in Fig. 2 in the previous section, are often about 50 micrometers at actual manufacturing sites. Therefore, relative positions between cameras, film and light sources have to be ten times more accurate to obtain images suitable for continuous defect detection.

Usually, it is relatively easy to precisely fix the relative position between the cameras and the light source. In practice, the position of the light source is allocated first and the alignment of cameras can be adjusted next by using three or five axis optical stages. However, conveying film with good precision in positions relative to the cameras and the light source is extremely difficult. Long products such as films warp easily and vibrate slightly during transportation. These phenomena have important effects on visual inspection. Therefore, large-scaled film transport devices and highly-skilled operation techniques are needed to carry out film feeding in actual production sites, yet there are many cases in which it is difficult to completely suppress deformation of the film.

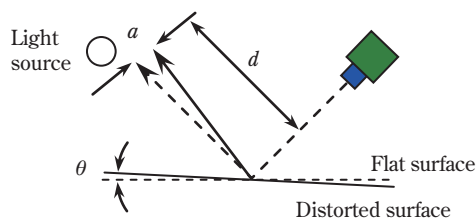
The influence of slight film distortion on observed images is described in Fig. 3 as an example showing the importance of the web handling. An example of an image under reflected light is given here. Many types of defects can be observed on-edge in the reflected



**Fig. 3** Film distortion and its adverse affect on observation of a defect  
Each lower plot shows intensity profile on a dashed line (line sensor view) in the upper image.

image of the light source, in other words in the boundary region of bright fields and dark fields. In Fig. 3 (a), the relative positions of the camera and the light source, an example of an observed image and the intensity profile at the defect position are shown for a case in which the film surface is maintained in a prescribed plane. In this case, only the defective area has higher intensity values compared to the peripheral region, so the defect can be extracted successfully. This is because the imaging position of the line sensor is aligned along the edge of the light source projected on the film. On the other hand, Fig. 3 (b) shows an example of an image and its intensity profile in the case where the film has slight distortion. In this instance, the image of the light source that ordinarily has a linear shape is severely distorted. Therefore, the edge of the light source image strays from the imaging position of the line sensor in the left half region. In addition, they cross in the right side region, so the light source is directly observed inconveniently.

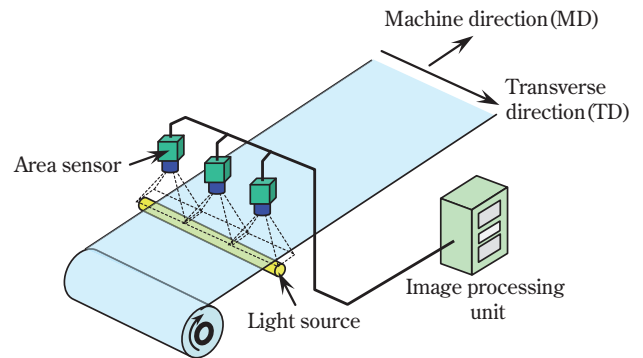
The tolerance of film distortion  $\theta$  is based on an allowable value  $a$  for the imaging position error from the image of the light source and the working distance  $d$ . In Fig. 4, for example, the allowable value for the film distortion is approximately  $\theta = \tan^{-1}(a/2d) \approx 0.007^\circ$  while the positioning tolerance  $a = 50 \mu\text{m}$  and the working distance  $d = 200 \text{ mm}$ . It is extremely difficult to keep the film surface flat within this range with normal web handling techniques.



**Fig. 4** Deviation of line sensor view due to film distortion

### Inspection Technique with Area Sensors

As a main target of our research, the overview of our web inspection technique using area sensors is described in this section. The configuration of the inspection system, in which the conventional line sensors are replaced by area sensors, is shown in Fig. 5.

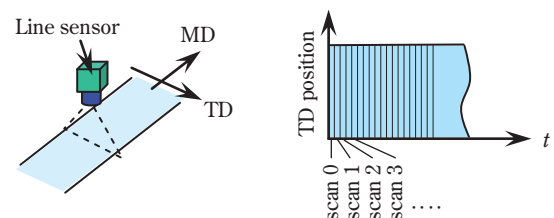


**Fig. 5** 2-dimensional web inspection system

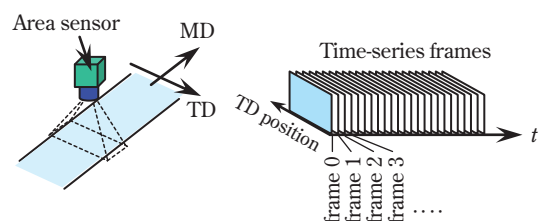
### 1. Comparison between line sensors and area sensors

Line sensors, as shown in Fig. 6 (a), output one-dimensional image signals repeatedly. Imaging across the entire area of film is possible by rolling the film at a fixed speed. Therefore, each defect has only one chance to be imaged when it passes under the scanning position of the line sensor. The scanning speed (number of imaging per unit time) of the line sensor is determined by the drive conditions for the camera. When a typical camera, for example, is driven by a clock frequency of 40MHz and a scanning rate (equivalent to exposure time per image) of 10,000 pulses, the images will be output at a speed of 4,000 scans per second.

Area sensors, in contrast, can output a two-dimensional still image (frame) in one exposure. Typically, motion images denote the time-series frame data captured continuously at a regular interval. Fig. 6 (b) represents



(a) 1D-images by using line sensor



(b) 2D-images by using area sensor

**Fig. 6** Comparison of image constructions

time-series frames conceptually. The number of frames output per unit time by the area sensor is called the frame rate, and it is usually expressed in frames per second (FPS).

## 2. Why area sensors are not used in web inspection

In most cases line sensors are used for in-line inspections of web products, mainly because the frame rate of area sensors is not sufficient for in-line usage.

Although the output rate per pixel (pixel clock) is approximately the same between line sensors and area sensors, the frame rate of area sensors is always one tenth or one hundredth of the scanning speed of line sensors. This is because area sensor images have 1 million pixels ( $1,000 \times 1,000$  or one megapixel) at least, much more than that of line sensor images, which are usually about  $10,000 \times 1$  pixels. As a consequence, the frame rate of area sensors is usually several dozen or a couple of hundred at best.

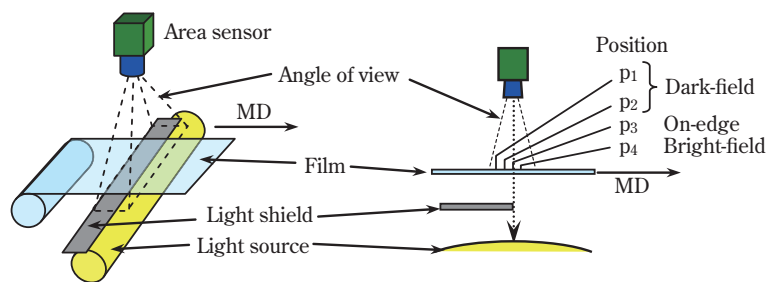
To use area sensors for web inspection, two-dimensional motion images must be acquired at a frame rate equivalent to the scanning rate of a line sensor, plus, image processing is supposed to be implemented in real time. Unfortunately, area sensors satisfying these requirements are not existing conventionally. In addition, image processing by software has limitations in

execution speed. Therefore, dedicated hardware is required to achieve real-time processing, despite extraordinary costs. For this reason, no reports related to web inspection with area sensors are available yet.

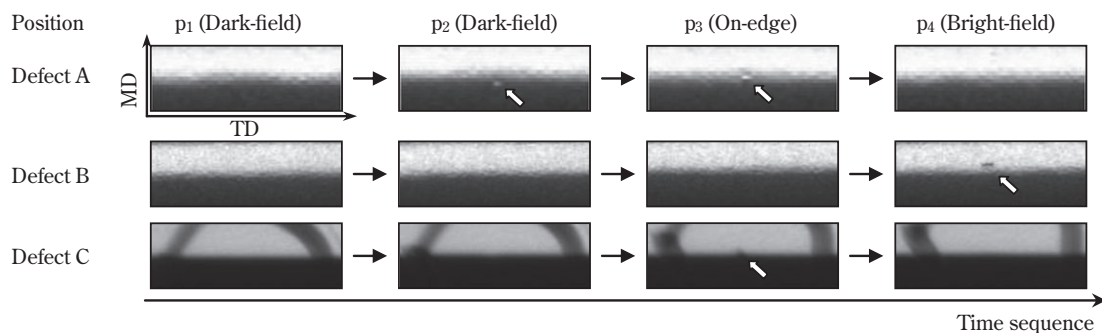
In recent years, it has become possible, to a certain extent, to develop image processing hardware by users. Therefore, applying area sensors to web inspection fields is promising in the future.

## 3. Advantage of using two-dimensional motion images for defect inspection

One of the great advantages of two-dimensional motion images is that variations in defect appearance can be observed over time. Fig. 7 (a) shows an example of device arrangement for obtaining two-dimensional motion images suitable for web inspection. The film is transported from left to right in the figure. A light shield is mounted to cover half the area of the light source so that the area sensor can implement dark field images at half of the area of the view and bright field images at the other half. With this arrangement, a defect being conveyed first comes into the dark field view and goes into the bright field area across the edge of the light shield, then passes out of sight. The images acquired during this motion contain vast defect patterns under different optical conditions from dark field to bright field. Fig. 7 (b) shows examples of actual



(a) Configuration of the optical system



(b) Observation of defects in 2D motion images

**Fig. 7** Examples of defect images by using an area sensor



defect observation, where characters  $p_1$  through  $p_4$  indicate the various positions in the field of view shown in Fig. 7(a). Position  $p_1$  and  $p_2$  correspond to the dark field region,  $p_3$  denotes the on-edge, while  $p_4$  refers to the bright field region respectively. Defect A can be observed from the dark field position  $p_2$  to the on-edge position  $p_3$ , but cannot be seen in the bright field position  $p_4$ . By contrast defect B can only be observed in the dark field position  $p_4$ . In addition, defect C cannot be observed at any position, but distortion of the edge can be observed when it passes the on-edge position. This defect C is difficult to detect by using conventional line sensors because of the effects of film warpage described in the previous section. This kind of defect is expected to be detected by using two-dimensional motion images, which include additional information such as temporal changes in edge distortion.

### The LCI Solution that Provides Clear Defect Images from Two-Dimensional Motion Images

In this section, we will introduce an image processing technology named “line composition and integration (LCI)”, which has been developed to extract intelligence involving defects from two-dimensional motion images with reliable sensitivity.

#### 1. Basic concept

In a two-dimensional image sequence, the information about a certain defect is decentrally-included in multiple continuous frames. Furthermore, which frame includes more information about the defect depends on the defect type, as described in sections 2 and 3. Therefore, all frames should be treated in order to detect more varied defects, instead of carrying out image processing on individual frames.

However, it is practically difficult to implement tradi-

tional image processing on entire frames, considering the enormous resources which need to be embedded into the image processing engine, and the unreasonable costs of application such as film inspection.

In this research, the authors attempted to propose a novel method to reduce the redundancy of image data by extracting just the defect information from the motion images. A conceptual diagram of this method is shown in Fig. 8. Rather than directly processing two-dimensional motion images (original images) output by the area sensor, LCI extracts defect information from continuous multiple frames and integrates it into a single line, and eventually outputs it to the image processing unit. This consolidated image is called an LCI image. With this operation, defect information that was distributed to multiple frames can be consolidated into one LCI image; therefore, the defect image obtained by the LCI method is clearer than those obtained by traditional methods. In addition, by limiting the target data to the LCI image, the amount of image data that must be processed within a unit time can be reduced to an identical amount of data as traditional line sensors.

#### 2. Principles of LCI

The procedure of LCI consists of three steps, namely, line composition, operator calculations and image integration as shown in Fig. 9. In the following, each procedure is described.

##### (1) Line composition

The operation of extracting the same line (row data) from each original frame and rearranging them in a time series is called “line composition.” The original image, shown in Fig. 9 (a), is sliced into line images. Each line is stored in structurally allocated memory blocks respectively, in order to generate a line composite image (b).

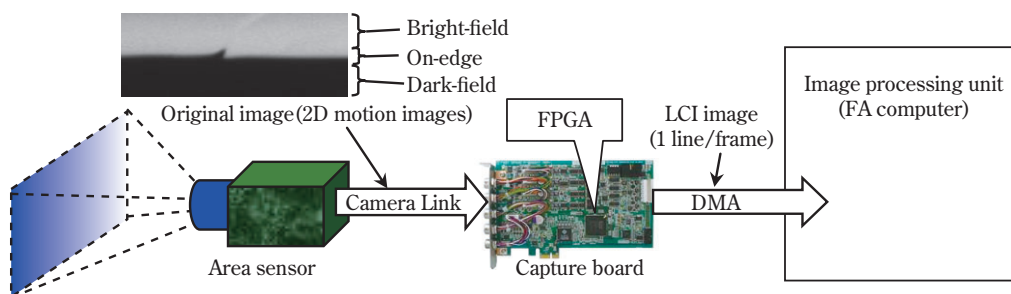
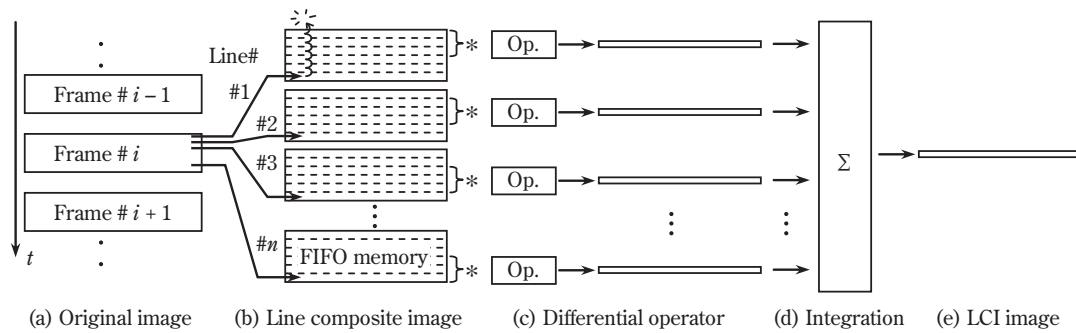


Fig. 8 Conceptual diagram about LCI



**Fig. 9** LCI procedure

With this operation, an image which is practically the same as the image scanned by a line sensor at the same position can be obtained. Multiple line composite images, obtained in this procedure, can be reckoned as they are obtained at different imaging positions against illumination by a distance equal to the camera resolution. In particular, under the optical arrangement in Fig. 7 (a), these images include various optical conditions from bright field to dark field.

### (2) Operator calculations

Appropriate operator calculations are carried out for each line composite image. The purpose is to cast intensity changes caused by defects as unsigned numbers before following the integration process. In the case of a differential operator, for example, absolute values of the gradient of the intensity profile should be used. The reason is that whether the intensity changes due to defects are positive or negative differs according to the optical conditions. Therefore, the phenomena that a certain defect would appear black in bright field images and would also appear white in dark field images often occur in actual sites. By using unsigned numbers, the drawback that these defect signals would counteract each other during integration process can be avoided.

### (3) Image integration

As the final image form, the LCI image is generated by accumulating the operator processed images and realigning changes in film position caused by conveying. The memory block storing each line composite image is FIFO (first-in, first-out) memory, and the imaging position on the film can be aligned among the line composite images by shifting the target region of operator calculation, shown by the character “}” in Fig. 9 (b). The LCI image is a single line image output for each frame by implementing this series of procedures.

## 3. Equipping of LCI algorithm

The LCI algorithm can be implemented via either a software method or a hardware method. However, from a practical standpoint for web inspection, two-dimensional motion images output at a high frame rate are necessarily processed in real time. Therefore, while execution by software is not feasible, hardware based implementation is desirable. In this research, we selected FPGA. The LCI algorithm was implemented by an FPGA mounted on a capture board as already shown in Fig. 8. According to experimental results, it is possible to separate the LCI from the camera and software, and this is useful for many occasions as a general purpose board with LCI function.

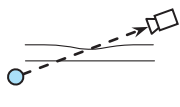
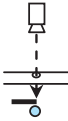
The LCI is able to generate images just by carrying time-series image processing like image separating, time delay and arithmetic operations. Therefore, its logic circuit is simple. However, because of the principle of the LCI algorithm which arranges the image data in a time series, the LCI requires vast resources (particularly FIFO memory). Normally, comparing with the expandable memory capacity of personal computers, the memory size installed in the FPGA has limitations. Therefore, image size (number of lines integrated), parallelism and other features must be selected suitably.

## Experimental

### 1. Example of observed images

In this section, observations of two different defect patterns on film surfaces are demonstrated. Each defect requires different observation methods to be detected. The characteristics of these defects are summarized in Table 1. For example, the slight concave defect can not be detected under any observation method described above. But, it could be visible just by seeing the distortion in a transmission image of the light source.

**Table 1** Defect samples

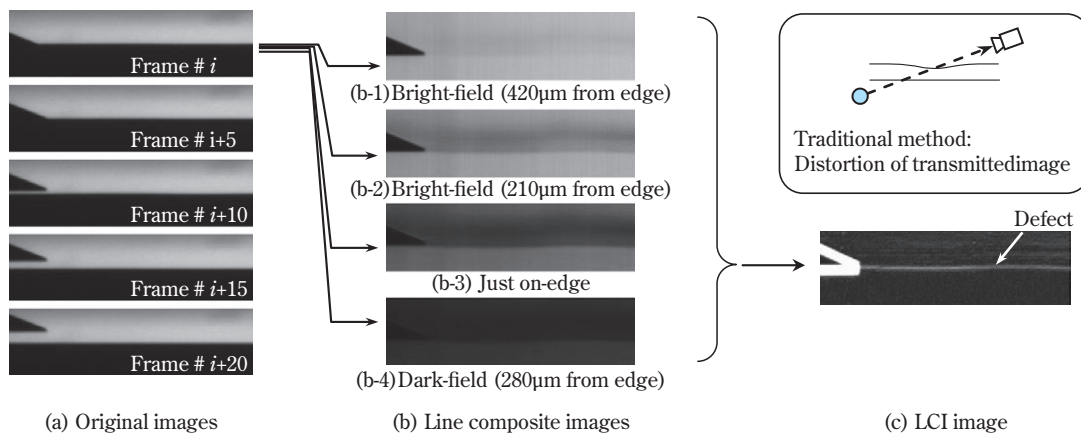
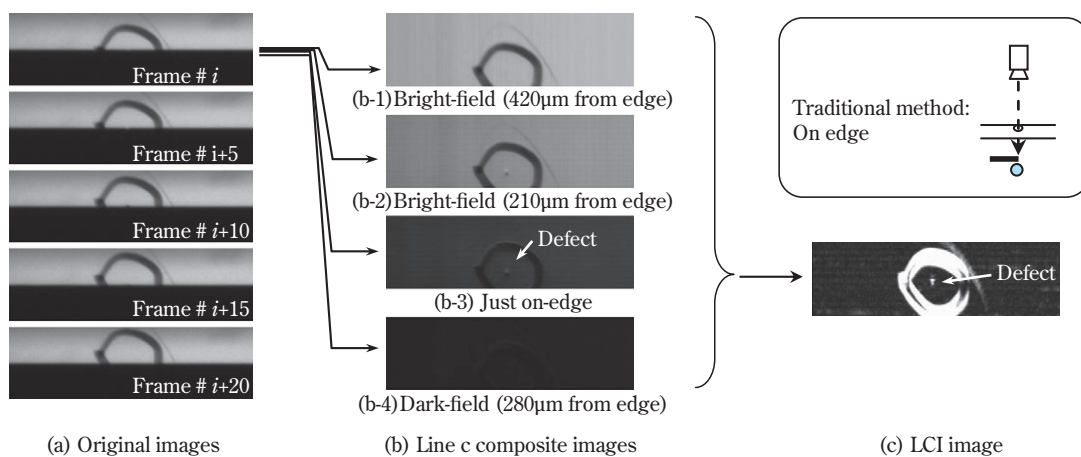
Defect type	Slight concave	Particle
Typical size	Height : 1 $\mu\text{m}$ Width : 1mm or more	Less than 100 $\mu\text{m}$ in diameter
Observation method	Distortion of transmitted image 	On-edge 

Observation examples of the defects are shown in Fig. 10 and Fig. 11. In these figures, part (a) shows some frames of the original images where defects are passing near the edge, but, they are not visible in these images. Some of the line composite images are shown in part (b). Though the defects are barely able to be

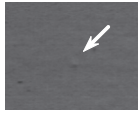
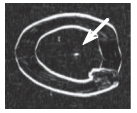

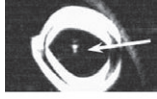

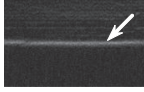
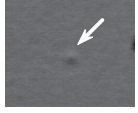
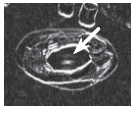
observed, the intensity difference compared with the normal region (the background of the images) is not sufficient. Part (c) in the figure shows an LCI image. In the LCI image, we can see the apparent brightness difference between the defect and the background. Although these defects require different observation methods for detection, both defects can be observed under the same optical conditions by using the LCI method.

## 2. Comparison to traditional method

Fig. 12 shows some defect images observed by traditional methods and LCI. The traditional observation method differs among these defects, because each defect requires different optical condition respectively. (Here, involving the traditional methods, the exposure time or lens aperture is adjusted individually to keep the image brightness within the dynamic range of the


**Fig. 10** LCI experimental result (Defect type: Slight concave)

**Fig. 11** LCI experimental result (Defect type: Particle)



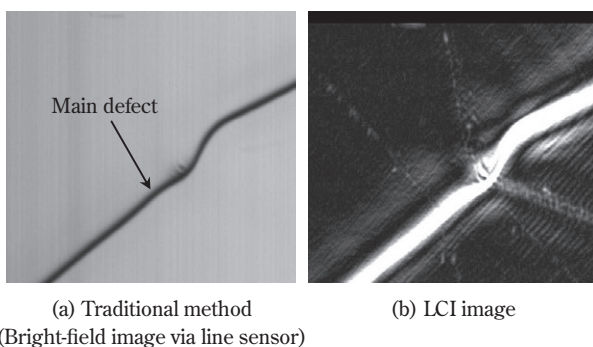
Defect and observation method	Traditional method	LCI image
Convex defect (Dark field)		
Particle 1 (On edge)		
Slight concave (Distortion of transmitted image)		
Particle 2 (Bright field)		

**Fig. 12** Comparison of defect images between LCI and traditional methods

camera.) In contrast, the observation conditions for LCI are fixed and are not varied for the types of defect. From these results, we can expect that with our approach it becomes possible to reduce the quantity of inspection devices in practice, while multiple devices are definitely needed in the traditional method.

### 3. Visualization of surface microstructure

Fig. 13 shows an example of the observation of a surface microstructure defect, which is another different defect type. This defect has a thread concavo-convex shape with roughly 10 micrometers depth as the main defect, and has widespread slight unevenness with 0.1 micrometer depth around it collaterally. Fig. 13 (a) shows a bright field image using a line sensor in one of the traditional methods. In this case only the main defect



**Fig. 13** An example of LCI image observed film surface with complex shape

is detected, and the microstructure in the vicinity cannot be observed. Next, Fig. 13 (b) shows an LCI image. Seeing this, we can see stripe patterned unevenness around the main defect. This result shows that observation of microstructures, which was difficult to be visualized with any conventional method, is possible by LCI. Usually, a three-dimensional measurement device, founded on the principle of optical interference for example, is needed to determine micro-geometry on a film surface. However, it is mechanically difficult to carry out precise three-dimensional measuring in-line, so these observations are limited to off-line sampling inspections. Visualization of microstructures over the entire surface is possible by monitoring LCI images, which suggests that the LCI can also be used for diagnosis and improvement of manufacturing processes.

### Optical Simulations

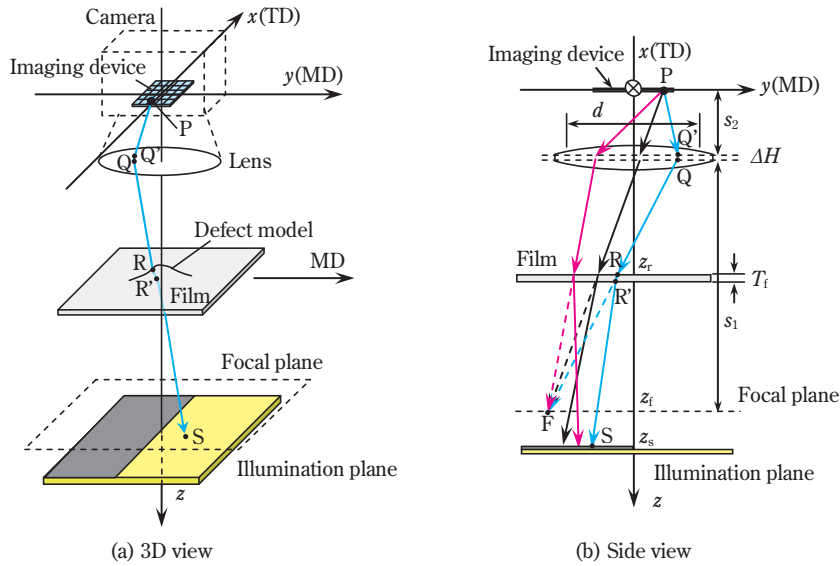
In this section, by performing ray tracing from the imaging plane through the film surface to the illumination plane, generation of computer graphics of defect images with LCI is to be discussed.

#### 1. Significance of image composition by simulation

It is important to evaluate the defect detecting performance of in-line inspection systems for practical usage. Generally, the detection capabilities are evaluated experimentally by using collected defect samples. However, it is not efficient to exhaustively carry out observational tests under the various arrangements of the camera, film and illumination. In addition, it is actually difficult to collect various sizes of actual samples containing all types of defects from products. Therefore, it would be more effective to analyze uncollectable defects via simulations. With this, it would be possible to interpolate incomplete experimental results, which could improve experimental efficiency.

#### 2. Definition of coordinate system

The coordinate system used in the simulations is defined as in Fig. 14. The  $z$  axis is the optical axis, and the imaging plane is defined by  $z = 0$ . The transverse direction (TD) of the film is  $x$ , and  $y$  indicates the machine direction (MD). An aberration-free single thick lens, which has distance between two principal points  $\Delta H$ , is considered here. (An aberration-free lens is accurate enough for our purpose for interpolation of



**Fig. 14** Coordinate system for LCI simulation

experimental results, and effective simulation results are obtained.) The film is considered to be a plane parallel plate with thickness  $T_f$ , and it is arranged on the plane  $z = z_r$ . The focal plane is represented by  $z = z_f$ , where  $z_f$  is uniquely determined from the imaging plane, lens position and lens parameters. The surface light source is arranged on the illumination plane  $z = z_s$ . Any brightness pattern can be represented by giving various intensity profiles to the light source on this plane. For LCI simulation, a light source model in which the region  $y < 0$  is shielded (letting the brightness value be zero) is used here.

### 3. Procedure for generating computer graphics

The computer graphics for the observed defect image can be generated by the following procedure. First of all, point P on the imaging plane is determined, then, a large number of rays from point P toward the inside of the lens aperture are set. Each ray launched from the same point P is headed toward the same focal point F on the focal plane  $z = z_f$  regardless of the incidence position Q of the lens aperture. Along the way, the rays incident to the film surface are refracted at the front and back surfaces, attenuate during their passage through the film and then keep on heading to the illumination plane. The point S indicates the position where each ray reaches the illumination plane. By accumulating the intensity of the light source for all rays launched from the same point P, the amount of light received at P is calculated. By repeating this

process over the entire region of the imaging plane, a two-dimensional image can be generated by the area sensor. Furthermore, continuous two-dimensional motion images are generated by repeatedly forming the two-dimensional still image as the film moves forward step by step by a distance corresponding to the film speed.

### 4. Ray tracing<sup>5), 6)</sup>

#### (1) Determination of imaging optics

The lens with focal length  $f$  and principal point distance  $\Delta H$  are considered. The size of each pixel on the imaging device is  $r_0$ . With this assumption, the optical arrangement is uniquely determined once the resolution of the image  $r$  [m/pixel] is fixed. Since aberration in the lens is not considered, all rays launched from the same point P on the imaging plane will be focused on the same point F ( $x_f, y_f, z_f$ ). The focal point F is given by the following formulas;

$$\text{magnification ratio} \quad M = \frac{r}{r_0} = \frac{s_1}{s_2} \quad (1)$$

$$\text{lens formula} \quad \frac{1}{f} = \frac{1}{s_1} + \frac{1}{s_2} \quad (2)$$

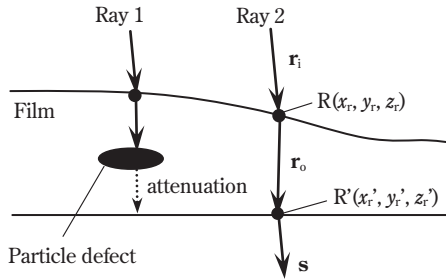
$$\left. \begin{aligned} x_f &= -M \cdot x_p \\ y_f &= -M \cdot y_p \\ z_f &= s_1 + s_2 + \Delta H \end{aligned} \right\} \quad (3)$$

where,  $s_1$  is the distance from the primary principal point on the lens object side to the focal plane, and  $s_2$  is

the distance from the imaging plane  $z = 0$  to the secondary principal point.

## (2) Effect of defects on the rays

Each ray reaches position R on the film surface, which is calculated from point Q on the lens and focal point F. If a defect exists around there, the ray will be attenuated by the defect inside the film (Ray 1), or its direction will alter at the film surface (Ray 2) as shown in Fig. 15. In the simulation, the light shielding effect is quantified by multiplying the brightness of the light rays by coefficient  $k$  ( $0 < k < 1$ ). In addition, refraction by the front and back surface is calculated by using a normal vector for the film surface at each position.



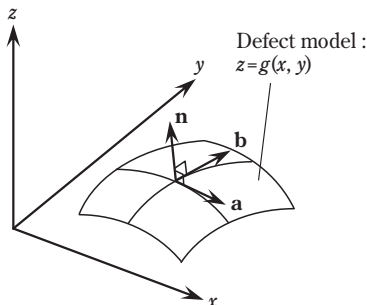
**Fig. 15** Variation of rays affected by defects

As one defect shape, for instance, the Gaussian function is defined as below,

$$z = g(x, y) = Ae^{-2\frac{x^2+y^2}{\sigma^2}} \quad (4)$$

where the height (or depth by negative values) of convexo-concave defect is expressed by the value of  $A$ , and planar defect size are expressed by  $\sigma$ .

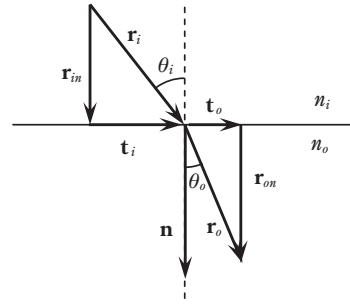
The normal vector on a surface  $z = g(x, y)$  at a point  $(x, y)$  is found as follows from the vector product of the tangent vectors in the  $x$  direction and  $y$  direction (see Fig. 16).



**Fig. 16** Defect model and its normal vector

$$\mathbf{n} = \left( -\frac{\partial g}{\partial x}, -\frac{\partial g}{\partial y}, 1 \right) \quad (5)$$

Next, the path of the ray through the film is calculated. The unit directional vector  $\mathbf{r}_i$  for the ray incident to the film surface from the air, the unit normal vector  $\mathbf{n}$  for the boundary surface at the incidence point and the unit directional vector  $\mathbf{r}_o$  for the light beam after refraction are expressed by equation (6) and shown by Fig. 17. Similarly, the refraction at the back surface from the film to the air could be calculated.



**Fig. 17** The change of ray direction at the medium boundary surface

$$\left. \begin{aligned} \mathbf{r}_i &= (x_i, y_i, z_i) \\ \mathbf{r}_o &= (x_o, y_o, z_o) \\ \mathbf{n} &= (x_n, y_n, z_n) \end{aligned} \right\} \quad (6)$$

The direction  $\mathbf{r}_o$  for the light beam after passing through the boundary surface is calculated by using the incidence angle  $\theta_i$  and the refractive indices of each material  $n_i$  and  $n_o$ , with the following equations, the vector representation of Snell's law;

$$\left. \begin{aligned} x_o &= \frac{n_i}{n_o} x_i + \left( S_o - \frac{n_i}{n_o} S_i \right) x_n \\ &= \mu x_i + \Gamma x_n \\ y_o &= \mu y_i + \Gamma y_n \\ z_o &= \mu z_i + \Gamma z_n \end{aligned} \right\} \quad (7)$$

where

$$\left. \begin{aligned} \mu &= n_i/n_o \\ S_i &= \mathbf{r}_i \cdot \mathbf{n}, S_o = \mathbf{r}_o \cdot \mathbf{n} \\ \Gamma &= S_o - \mu S_i \\ &= \sqrt{1 - \mu^2 + \mu^2 S_i^2} - \mu S_i \end{aligned} \right\}$$

By tracing the ray path at the front and back surface of the film with equation (7), we can find the position of the ray passing through the film and the direction of the ray (point R' and vector  $\mathbf{s}$  in Fig. 15).

(3) Calculation of point of arrival of the ray on light source surface

Point S, the arrival position of the ray at the surface of light source, can be calculated by point R' and vector  $s$ , which were found in the previous section. However, because of the diffraction limit, the ray left point P on the imaging surface does not focus on a single point S on the surface of the light source. Normally, when the light is concentrated on an image forming surface, the spot diameter of light that leaves a single point is given by the following equation, even with a lens that has no aberration.

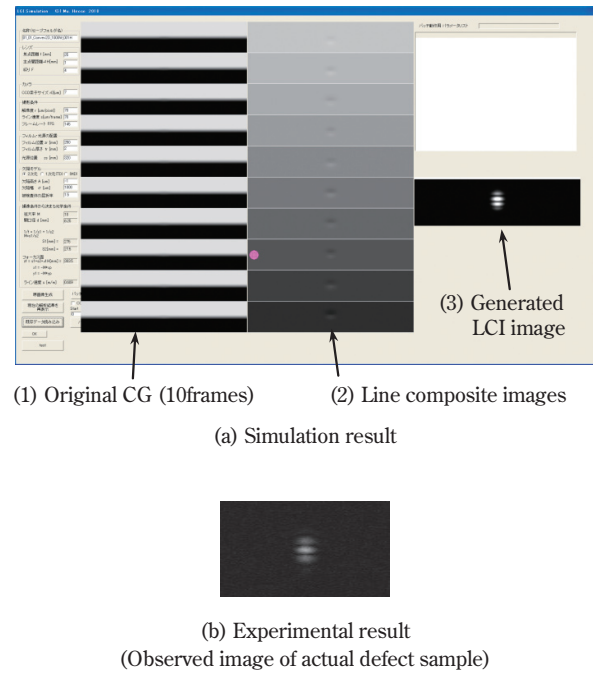
$$d_s = 2 \times 1.22f\lambda/d \quad (8)$$

Where,  $\lambda$  is the wavelength of the light source,  $f$  the focal length of the lens and  $d$  the aperture. In addition, since in this simulation the light source is arranged according to the distance between the image forming surface and light source surface, regardless of the focus position of the lens, the spread of the spot caused by diffraction needs to be corrected. The intensity of light received at point P for this ray is calculated using the average brightness value for the spot region centered on point S. The total intensity of light received at point P can be found by adding these intensity values for all light rays leaving point P.

## 5. Results of simulation

Fig. 18. shows observed images generated using ray tracing simulation and the LCI image. In this example, a convex defect model arising on the front surface of the film is used. The shape of the defect is expressed by the Gaussian function, with a height of  $1\mu\text{m}$  and a width of  $1\text{mm}$  ( $2\sigma$ ). In the figure, (1) Original CG (original images) are the two-dimensional motion images repeatedly generated while shifting the film position a certain distance in the MD direction corresponding to the line speed. Though about 100 frames of original images are needed to generate one actual LCI image, the representative ten frames are displayed in this figure. Next, (2) Line composite images are an extraction of the same line from continuous frames in the original images which are rearranged in a time series. (3) The LCI image is generated by integration after carrying out the operator calculations on these line composite images.

For comparison, an experimental result is shown in Fig. 18 (b). An actual defect with substantially identical



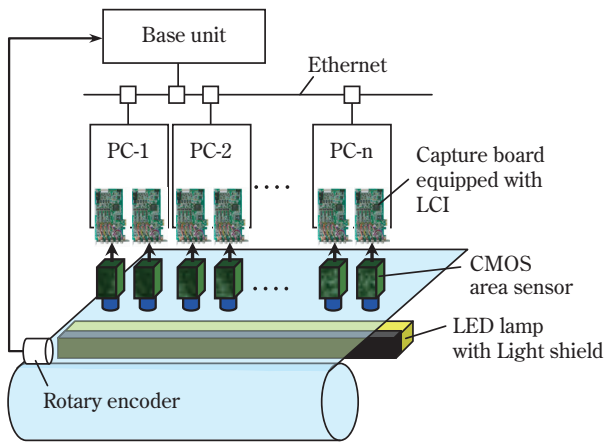
**Fig. 18** Comparison between simulation and experimental result  
Defect model: Convex defect (defect height  $1\mu\text{m}$ , defect width  $1\text{mm}$ )

shape as the model is observed by using the image processing board with LCI function. Analyzing these results, we can see that computer graphics similar to the image of the defect actually acquired is generated by the simulation.

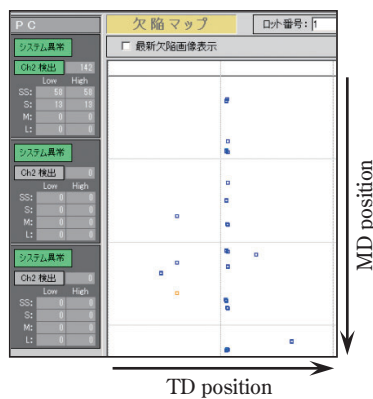
## Development of In-Line Web Inspection System

Fig. 19 shows the proposed framework of the in-line web inspection system.

The processing core consists of one personal computer (PC) as a parent terminal and multiple child PCs working under the control of the parent terminal. The child PCs are equipped with image capture boards. Each capture board is loaded with the LCI algorithm via an FPGA chip. For each frame acquired from the area sensors by DMA on the child PCs, LCI images can be generated and transmitted. Therefore, the images received by the child PCs are just one line per frame, thus, although the inspection device handles two-dimensional motion images, it is still possible to inspect roughly the same data amount as a conventional line sensor system. Each child PC extracts defect information from the LCI images, meanwhile, and transmits



(a) Configuration of in-line inspection system



(b) An example of defect detection map

**Fig. 19** In-line web inspection system by using area sensors equipped with “LCI technology”

them to the parent PC. The parent PC does not carry out image processing. Designed without an image processing function, the parent PC merely generates a synthetic defect map based on the defect information collected from the child PCs. Plus, it carries out operations such as display, warning, storage and analysis of inspection data.

LED illumination for image processing was used for the light source, and a light shield plate was set up on the surface of the light source to provide a bright field region and a dark field region. A CMOS area sensor was selected for the cameras. CMOS sensors are able to set the image capture region as desired and are suitable for LCI. Since the position of the cameras and their resolution are fixed, the world coordinates (meaning the absolute position on the film) in the TD direction can be easily obtained from the image.

A rotary encoder is used for obtaining world coordinates in the MD direction. (A rotary encoder is a signal

generating device that outputs a certain number of pulses per rotation, and is generally used in order to measure distances for a continuously fed web-shaped product.)

As described above, this inspection device can be achieved with an equipment configuration substantially the same as a conventional web inspection device based on line sensors. Two-dimensional image processing should be installed in a hardware device, except for this, there is no need for special web-handling devices or special cameras, image processing engines, etc. With this great advantage, we can conveniently replace and improve the existing inspection devices.

Fig. 19 (b) shows an example of a defect map generated from real film inspection. Besides the above, this inspection system can pop up and display defect information maps through a mouse operation, and can also classify all detected defects by size, as well as create inspection databases and run other functions. In addition, there is also an option to offer a marking unit for defect locations.

## Conclusion

An in-line web inspection technology based on two-dimensional motion images is introduced. Using area sensors for imaging devices enables the changes in defect appearance that could not be obtained by traditional line sensors to be detectable. The authors established a novel image processing algorithm called LCI, which extracts defects from the motion images. The authors also achieved a real-time two-dimensional motion image processing system embedding the LCI algorithm into a capture board. Several experimental results indicated that defects which are undetectable by traditional methods could be detected by our approach. Computer graphics for LCI are generated by ray tracing simulations, and they showed good agreement with experimental results. We discussed the fact that through the joint use of experimental results from a limited number of defect samples and computer graphics, it is possible to interpolate test data, making it possible to optimize optical arrangements and efficiently evaluate inspection performance. Furthermore, we developed an in-line web inspection system based on this technology. The experimental results showed that it has sufficient inspection ability under actual film manufacturing conditions.



## References

- 1) Sangyo-yo camera no erabikata tsukaikata, Nihon Kougyou Syuppan (JAPAN INDUSTRIAL PUBLISHING CO., LTD.), (2012).
- 2) Machine Vision Lighting Kiso-hen (Machine Vision Lighting Basic Level), Nihon Industrial Imaging Kyokai (Japan Industrial Imaging Association), (2007).
- 3) Web-handling no kisoriron to ouyou, Kakou Gijutu KenkyuKai (Converting Technical Institute), (2008).
- 4) Hirose, Vision Gijutu no Jituriyou Workshop (Vision Engineering Workshop), (2009), p.223.
- 5) F. Jenkins and H. White, "Fundamentals of Optics", McGRAW-HILL (1957).
- 6) Hiakri Kiki no Kougaku I, Optomechatronics Kyokai (JAPAN OPTOMECHATRONICS ASSOCIATION), (1988).

## PROFILE



*Osamu HIROSE*

Sumitomo Chemical Co., Ltd.  
Industrial Technology & Research Laboratory  
Senior Research Associate  
Ph.D. in Engineering



*Maya OZAKI*

Sumitomo Chemical Co., Ltd.  
Industrial Technology & Research Laboratory  
Researcher